Research article Rapports De Pharmacie Vol.4 (1), 2018, 437-449
ISSN: 2455-0507

BOX-BEHNKEN DESIGN FORMULATION OPTIMIZATION AND IN VITRO CHARACTERIZATION OF RUTIN -LOADED PLA NANOPARTICLES USING DESIGN-EXPERT SOFTWARE

Lim Khian Giap, Jaya Raja Kumar

[1]*Research student, Asian Institute of Medicine, Science and Technology (AIMST) University, Bedong 08100, Kedah, Malaysia*

[2]*Unit of Pharmaceutical Technology, Faculty of Pharmacy, Asian Institute of Medicine, Science and Technology (AIMST) University, Bedong 08100, Kedah, Malaysia*

ABSTRACT

This study aims to prepare and optimize rutin-loaded nanoparticles using factorial design. The effect of major preparation variables, amount of drug, amount of polymer and sonication frequency on particle size, encapsulation efficiency, cumulative drug release (CDR) at 12th hour and polydispersity index (PDI) are studied with factorial design. Amended emulsification method was used to fabricate nanoparticles by using poly (L-lactide), which is biodegradable. Various parameters of nanoparticles were characterized which include particle size, encapsulation efficiency, cumulative drug release at 12th hour and polydispersity index. Scanning Electron Microscope (SEM) was employed to study the morphology of the prepared nanoparticles. FTIR studies were performed to assess the interaction between the excipients used and the drug due to its nature. The ideal formulation has a particle size of 240.596nm, encapsulation efficiency of 70.376 %, CDR at 12th hour of 78.978 % and PDI of 0.2926. SEM results indicate that the nanoparticles are spherical in shape. On the other hand, FTIR results showed that the components used in formulating the nanoparticles are compatible.

Keywords: Rutin, High performance liquid chromatography, PLA nanoparticles, Probe sonicator, Factorial design

INTRODUCTION

Rutin is a flavonol glycoside encompassed the flavonol quercetin and the disaccharide rutinose. It is also known as (2-(3,4-dihydroxyphenyl)-4,5-dihydroxy-3-[3,4,5-trihydroxy-6-[(3,4,5-trihydroxy-6methyl-oxan-2-yl)oxymethyl]oxan-2- yl] oxy-chromen-7-one), quercetin-3-rutinoside or sophorin. It is a polyphenolic compound which is extensively occured in higher plants. Rutin has prominent oxidant scavenging properties like scavenging OH radical, superoxide radical, and peroxyl radical. To add on, it also shows pharmacological activities, for instance vasoactive, antiallergic, anti-inflammatory vasoactive, antitumor, antibacterial, antiviral and anti-protozoal properties. Rutin provides a pro over myricetin, quercetagenin and other flavonoids in the sense that it can act as a prooxidant agent and catalyze oxygen radical production. So, it can be considered as a potential but non-toxic and non-oxidizable molecule. Ironically, the con of the molecule is its poor water solubility which leads to poor bioavailability and pharmacological action.

Address for correspondence:
Lim Khian Giap,
Research student,
AIMST University,Bedong
Semeling, Kedah,
Malaysia- 08100

Hence, it poses some limitations on pharmaceutical application, specifically for oral use.[1]

A number of drug delivery systems were proposed for the entrapment of this active compound with the aim of improving its pharmacological activity. Namely, vesicles made up of sorbitan monostearate and polyethylene glycol fatty acid esters were investigated for the rectal delivery of rutin [2] while rutin-loaded ceramide liposomes embedded in a hydrogel were used to obtain an efficacious transdermal delivery [3]. Other devices were also used for the encapsulation of rutin, for instance mesoporous silica nanoparticles [4], nanoemulsions [5], micelles [6] and nanocrystals [7].

The properties of nanoparticles can be used to improve the pharmacological activity of rutin thus achieving a nanoformulations boasting long-term activity. To this end, rutin-loaded nanoparticles were experimentally prepared and characterized using factorial design.

MATERIALS AND METHODS

Materials:

Acetone was purchased from EMSURE, rutin was purchased from (Sigma-Aldrich Co), dichloromethane (DCM) was procured from (ACI Labscan), poly (L-lactide) was purchased from (Sigma-aldrich Co), potassium bromide (KBr) was purchased from (Nacalai Tesque) and

dimethylformamide was procured from (EMSURE). Deionized double-distilled water was used throughout the study.

Methods:

Preparation of rutin Nanoparticles:

Rutin-loaded PLA nanoparticles were formulated by using the single emulsion-solvent evaporation technique. [8] with minor modifications. Briefly, 50-100 mg of PLA polymer was dissolved in 1.5ml of dichloromethane (DCM) in a glass tube and vortexed for 5 min. Then 10 -20 mg of rutin powder was added to the 1ml of DMF solvent and polymer/solvent mixture and allowed to dissolve for 30 min, with intermittent vortexing. The organic phase containing PLA and rutin was rapidly added drop wise into a glass tube containing 1% of PVA in an aqueous solution by using a probe sonicator and mixture were subjected to sonication for 5 minutes at 50 amplitude in an ice - water bath (Qsonica Q55 Sonicator, USA), the resulting fine (O/W) emulsion was immediately placed on magnetic stirrer under vigorous stirring. Dichloromethane was then evaporated from the droplets under magnetic stirring at 1000 rpm for 3 hrs. To separate the nanoparticles from the continuous phase and residual solvent, first, rutin-PLA nanoparticles were centrifuged (Beckman Coulter Avanti J-26S XPI centrifuges) and the supernatant was discarded. The NPs were washed 2 times. Finally, the sample was lyophilized (Thermo Scientific-SuperModulyo 230, USA).

IN-VITRO EVALUATION

Particle size and polydispersity index (PDI):

The samples of rutin loaded PLA nanoparticles were diluted with distilled water for determination of particle size while polydispersity index was determined using Anton Paar Malaysia-Litesizer 500. Each measurement was done in triplicate.[9]

Encapsulation efficiency (EE):

In order to determine the encapsulation efficiency of rutin loaded nanoparticles, the difference between the total amount of rutin and total amount of free drug present was calculated. The HPLC was carried out at a flow rate of 1.0 ml/min using a mobile that is phase constituted of acetonitrile, 10mm AA: ACN (50:50, v/v), and detection was made at 370nm. The mobile phase was prepared daily, filtered through a 0.45µm. RP HPLC chromatographic separation was performed on a Shimadzu liquid chromatographic system equipped with a LC-20AD solvent delivery system (pump), SPD-20A photo diode array detector, and SIL-20ACHT injector with 50µL loop volume. The LC solution version 1.25 was used for data collecting and processing (Shimadzu, Japan).

EE was calculated using the equation: EE (%) = (total drug-free drug)/total drug [10]

Percentage of cumulative drug release:

The in-vitro release profiles rutin loaded PLA nanoparticles were determined using USP Apparatus II, with a 0.5 micrometer mesh. 1 g of rutin loaded PLA nanoparticles from the prepared nanoparticles was transferred to a phosphate buffer pH 6.8 in a receptor medium of 400ml containing 15 % methyl alcohol. Sink condition was maintained at 37°C ± 0.5°C with continuous stirring at the speed of 100 rpm. About 5ml of the sample was withdrawn at different time intervals and an equivalent volume of phosphate buffer solution was replaced into the beaker. The withdrawn samples were filtered through a 0.2 micrometer membrane. Next the concentration of drug in the medium was determined by using HPLC method.

RESULTS AND DISCUSSION

Experimental design:

The positive results of rutin nanoparticles formulations were described in this research study. Rutin (A), PLA (B) and frequency (C) were acknowledged as the most critical variables affecting the particle size, encapsulation efficiency %, CDR at 12^{th} hour, and polydispersity index (PDI) via the initial trials. In the midst the existing design methods, the Box-Behnken (BBD) possess decent design characteristics, minute collinearity and is rotatable or nearly rotatable. Some other approaches may be insensitive to missing data or may have orthogonal blocks. These cause them for not well in foreseeing at the corners of the design space. BBD is fit for discovering quadratic response surfaces and structuring second order polynomial models. It is composed of virtual center points in which the set of points reclining at the center of individual border of the multi-dimensional cube.

According to BBD, seventeen runs were indispensable for the response surface approach. The factor permutations which gave different responses are illustrated in Table 1. Obviously, all the dependent variables are reliant on the chosen independent variables. This can be inferred from a broad variation between the 17 runs. Data were evaluated by Stat-Ease Design-Expert software (DX11) to acquire analysis of variance (ANOVA), regression coefficients and regression equation. Mathematical relationship created via multiple linear

regression analysis for the studied variables are stated in Table 2.

Table -1: Factorial design of rutin nanoparticles formulations

Run	F1 A: Rutin	F2 B: PLA	F3 C: Frequency	R1 Particle size (nm)	R2 Encapsulation efficiency (%)	R3 CDR at 12^{th} hour (%)	R4 PDI
1	20	50	50	235	59.32	75.11	0.316
2	10	75	60	251.37	70.14	78.46	0.261
3	10	75	40	253.44	71.65	78.14	0.417
4	20	100	50	258.41	75.22	83.82	0.412
5	15	75	50	241.63	70.88	79.01	0.292
6	10	100	50	258.13	75.17	83.09	0.401
7	20	75	60	252.02	72.56	78.93	0.403
8	15	75	50	240.15	70.01	78.91	0.291
9	15	75	50	241.04	70.41	78.84	0.297
10	15	75	50	241.09	70.37	78.99	0.291
11	10	50	50	240.43	58.16	75.49	0.348
12	15	75	50	239.07	70.21	79.14	0.292
13	15	100	60	259.48	74.05	83.82	0.411
14	15	50	60	233.61	58.18	75.16	0.315
15	15	50	40	240.01	58.41	75.05	0.317
16	20	75	40	252.97	70.71	78.17	0.256
17	15	100	40	258.17	75.39	83.46	0.431

Table-2: Regression equation for the response

Response Regression equation
R1= +240.60-0.6212A+10.64B-1.01C+1.43AB+0.2800AC+1.93BC+6.01A^2+1.38B^2+5.84C^2
R2= +70.38+0.3363A+8.22B-0.1537C-0.2775AB+0.8400AC-0.2775BC+0.6745A^2-4.08B^2+0.2145C^2
R3= 78.98+0.1063A+4.17B+0.1937C+0.2775AB+0.1100AC+0.0625BC-0.2740A^2+0.6735B^2-0.2790C^2
R4= +0.2926-0.0050A+0.0449B-0.0039C+0.0107AB+0.0758AC-0.0045BC+0.0212A^2+0.0554B^2+0.0205 C^2

The normal % probability plot of the externally studentized residuals verified the data normality. The residuals distribute normally in the case of points lie in a straight-line pattern on the plot as demonstrated in Figure 1a,b,c and d.

Graph of externally studentized residual against predicted values was plotted to examine the idea of steady variance, as portrayed in Figure 2a,b,c and d. The studentized residuals are positioned by dividing the residuals by their standard deviations. R1, R2, R3 and R4, the points are disseminated in the range of detection limits - 4.82 to + 4.82.

Both Residuals vs. Predicted and Residuals vs. Run were distributed ununiformly. It is indicated that the model is apt for use and can be used to recognize the optimal parameters. The outcomes of R1 to R4 were quite satisfactory as shown in Figure 3a,b,c and d . Besides, low discrepancies are designated as the observed and predicted data establish a high extent of correlation.

λ is the transformation factor selected as it intensifies the log-probability function. The maximum possibility estimate of λ corresponds to the value for which the squared sum of errors from the suited model is at least. The λ value can be concluded by fitting various λ values and picking the value conforming to the least squared sum of errors. Graphical method can also be employed to choose the λ value from the Box-Cox normality plot. Value of λ = 1.00 specifies that there is no need of transformation and the results produced are similar to authentic data revealed in Figure 4a,b,c and d.

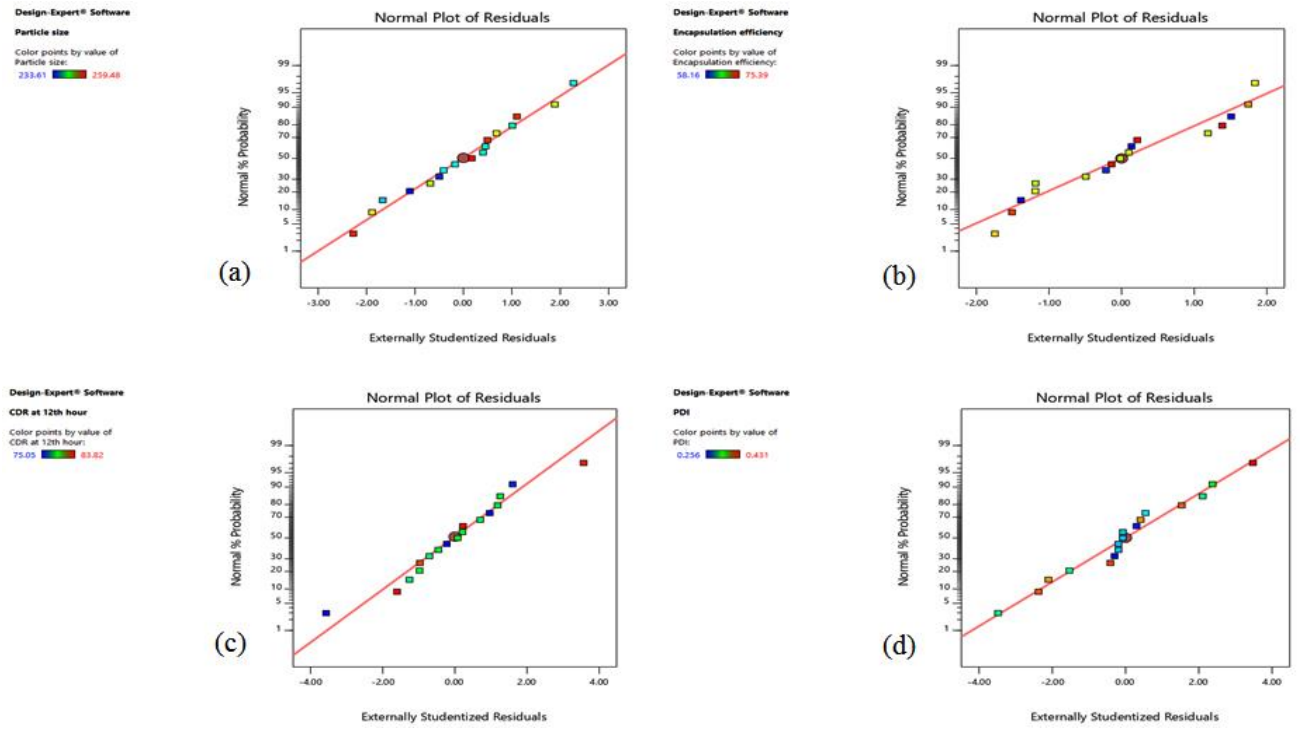

Figure-1: (a) Normal % probability plot of the externally studentized residuals (R1). (b) Normal % probability plot of the externally studentized residuals (R2). (c) Normal % probability plot of the externally studentized residuals (R3). (d) Normal % probability plot of the externally studentized residuals (R4)

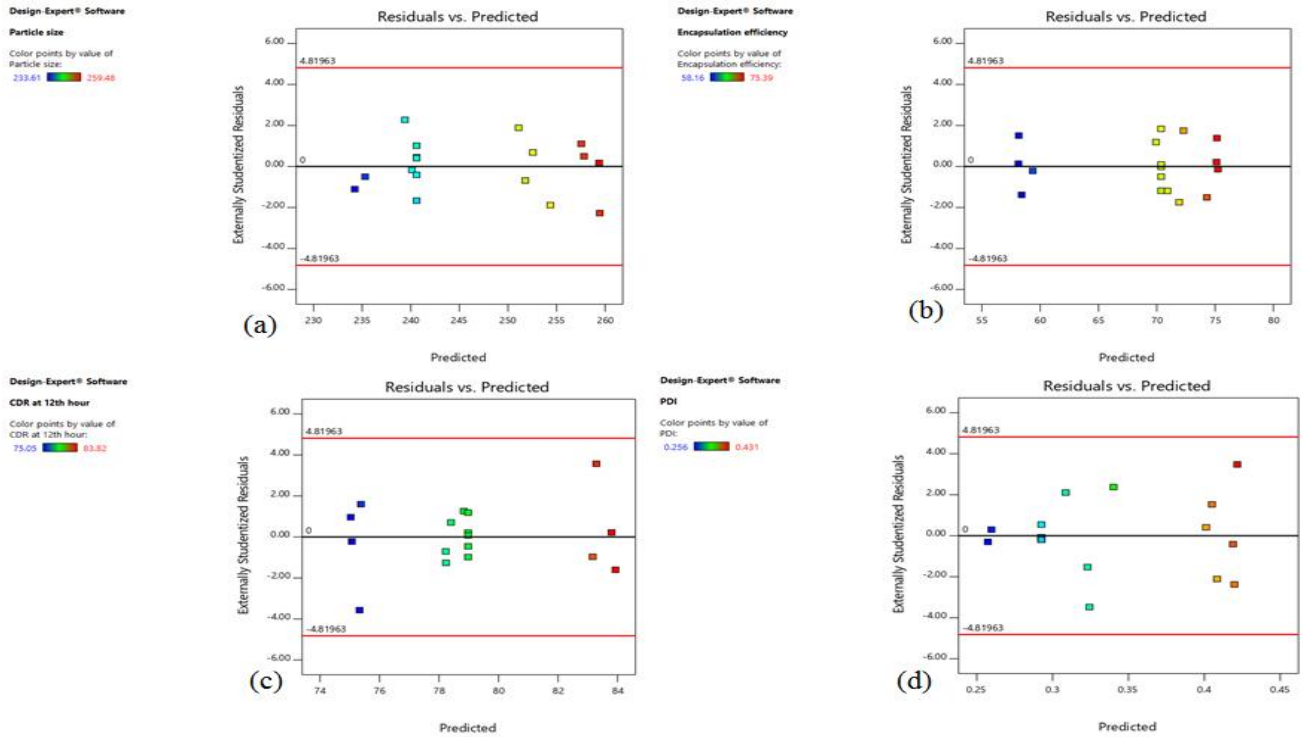

Figure-2: (a) Residuals vs. Predicted (R1). (b) Residuals vs. Predicted (R2). (c) Residuals vs. Predicted (R3). (d) Residuals vs. Predicted (R4).

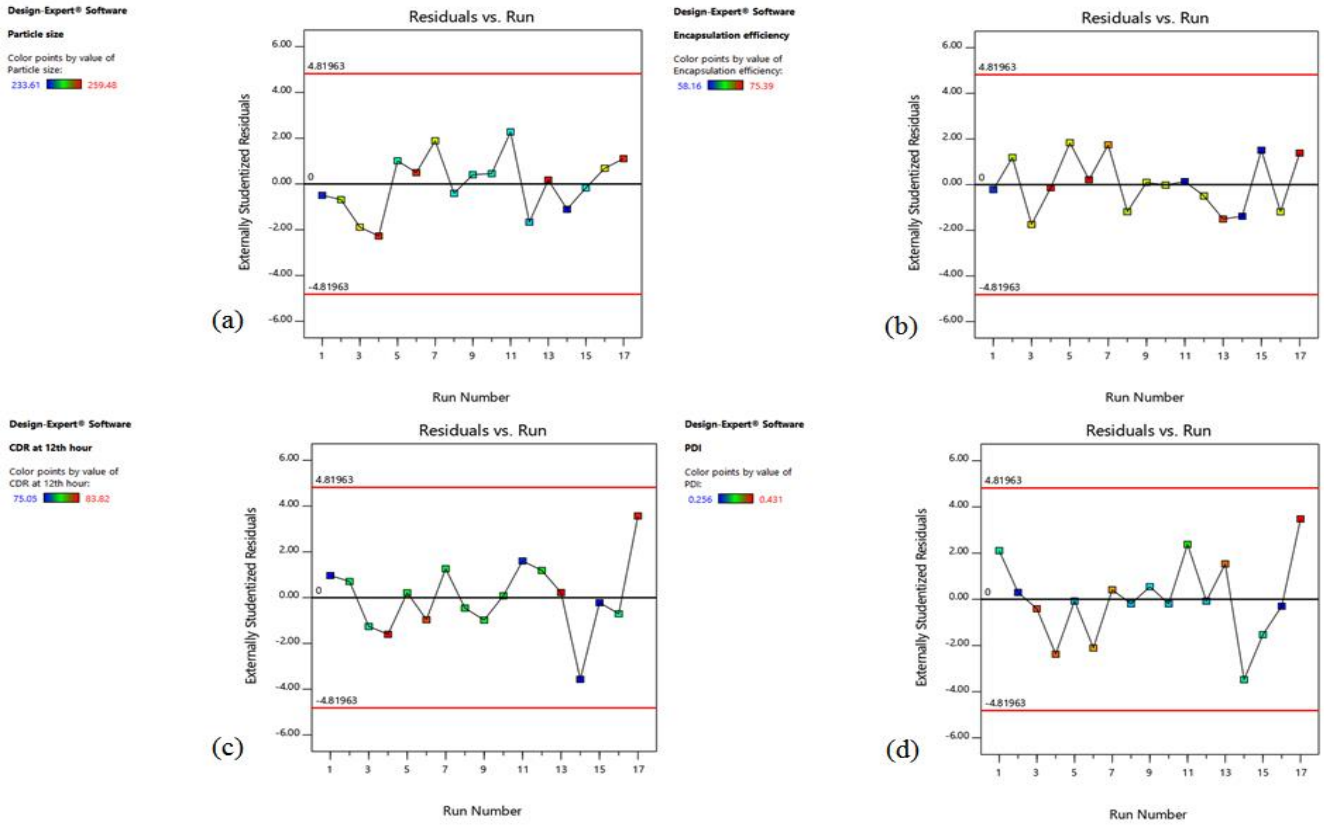

Figure-3: (a) Residuals vs. Run (R1).(b) Residuals vs. Run (R2).(c) Residuals vs. Run (R3). (d) Residuals vs. Run (R4)

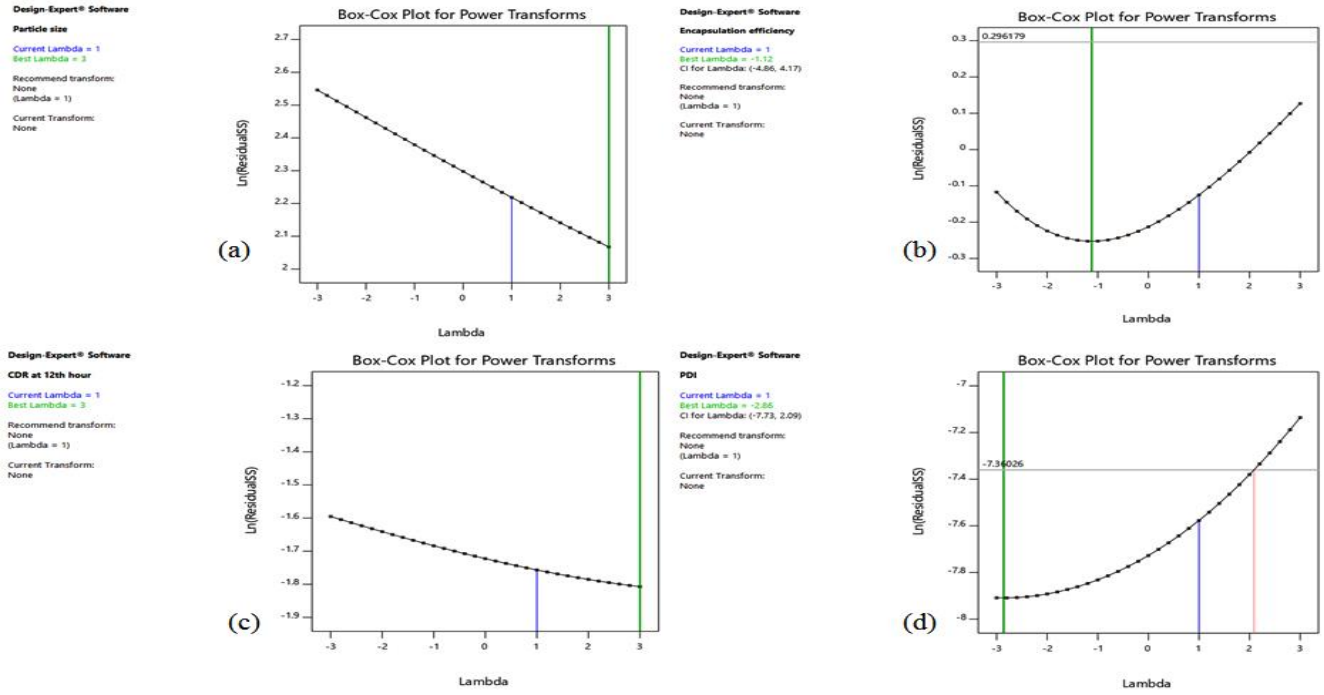

Figure-4: (a) Box-Cox Plot (R1). (b) Box-Cox Plot (R2). (c) Box-Cox Plot (R3). (d) Box-Cox Plot (R4).

Rutin nanoparticles have the particle size in between 233.61–259.48nm as shown in Table 3. A good correlation coefficient (1.000) is shown in the factorial equation for particle size and the model is

significant due to the Model F value of 107.54. "Prob> F" values of less than 0.0500 suggest that model terms are significant. A, C, AB, A^2 and C^2 are important model shown in Table 8. The Lack of Fit F-value of 1.70 implies the Lack of Fit is not significant relative to the pure error. There is a 30.36% chance that a Lack of Fit F-value this large could occur due to noise. Outcomes of the equation specify that the effect of Rutin (A) and Frequency (C) are more prominent as compared to B. The effect of the main and interactive consequences of independent variables on the particle size was clarified using the perturbation and 3D response surface plots. Main effects of each A, B and C on particle size are revealed in 5a. All of the variables possess interactive effects on the response R1. For illustrating the effects of interaction among independent variables of the response R1, the 2D response surfaces, 3D contour plots, 3D cube plot and 2D Interaction plot of the response R1 are presented in Figure 5b,c and d . The degree of the interaction between different factors is portrayed by the shapes of response surfaces and contour plots.

Table- 3: ANOVA results of the quadratic model for the response particle size (R1)

Source variations	Sum of Squares	DF	Mean Square	F Value	p-value Prob> F	
Model	1270.69	9	141.19	104.54	< 0.0001	significant
A-Rutin	3.09	1	3.09	2.35	0.1690	
B-PLA	906.10	1	906.10	690.14	< 0.0001	
C-Frequency	8.22	1	8.22	6.26	0.0408	
AB	8.15	1	8.15	6.21	0.0415	
AC	0.3136	1	0.3136	0.2389	0.6400	
BC	14.86	1	14.86	11.32	0.0120	
A^2	152.31	1	152.31	116.01	< 0.0001	
B^2	8.04	1	8.04	6.13	0.0425	
C^2	143.58	1	143.58	109.36	< 0.0001	
Residual	9.19	7	1.31			

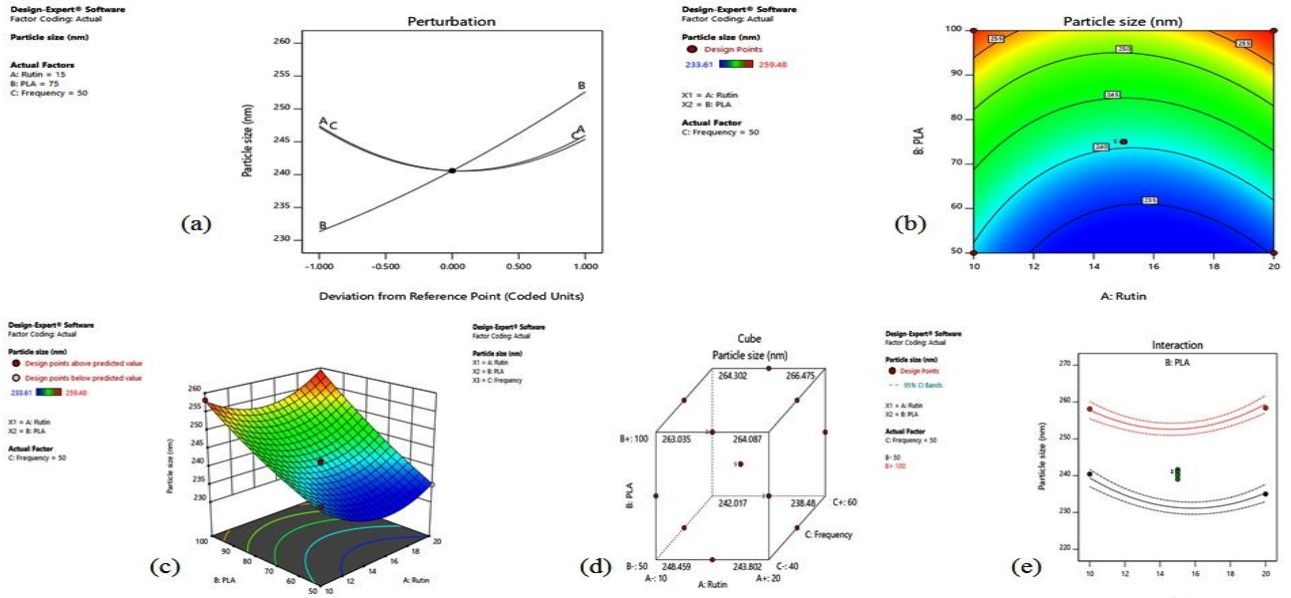

Figure-5: (a) Perturbation plot showing the main effect of Rutin (A), PLA (B) and Frequency (C) on particle size (R1). (b) 2D response surface plot presenting the interaction between the rutin and PLA affecting the particle size (R1). (c) 3D response surface plot presenting the interaction between the rutin and PLA affecting the particle size (R1). (d) 3D cube plot of Box-Behnken design (R1). (e) 2D Interaction plot presenting the interaction between the rutin and PLA affecting the particle size (R1).

R-squared is the coefficient of determination. Since it is a ration of the fraction of the total squared error, the value of R^2 ranges from zero to one. It is better if the value is closer to one. Nevertheless, a large value of R^2 does not certainly denote a good regression model. Adding a variable to the model will always

increase, regardless of the statistical significance of the additional variable, R^2 will be increased if a variable is added into the model. Hence, it is not necessary that models with large values of R^2 to CDR will have good predictions of new observations or estimates of the mean response. To shun this bewilderment, the Adjusted R-squared statistic is crucial in which its value falls if pointless variables are incorporated. The existence of extraneous terms can be implied when the two statistics are used together in the computed model which a large difference between the values of R^2 and Adj-R^2 is greater than 0.2. Residual is the difference in the amount of estimated output and the real output. Predicted Residual Error Sum of Squares (PRESS) is a measure of the extent of the model suits individual aspect in the design. Predicted R^2 can be calculated by PRESS. Adeq Precision measures the signal to noise ratio. A desirable ratio is of larger than 4. "Adeq precision" showed (R1, R2, R3, R4) was 168.19, 293.08, 43.95 and 87.38 shows sufficient signal individually. This model can be benefitted to navigate the design space. These statistics are employed with an intention of avoiding over suiting of model.

The mathematical model made for encapsulation efficiency % (R2) was observed to be substantial with F-value of 543.18 ($p < 0.0001$) and R^2 value of 0.9986. The independent variables A and C the quadratic term of A^2 pose major effects on the encapsulation efficiency. The model is significant as the P-values less than 0.0500. This is revealed in Table 4. The Lack of Fit F-value of 1.49 implies the Lack of Fit is not significant relative to the pure error. There is a 34.51% chance that a Lack of Fit F-value this large could occur due to noise. Non-significant lack of fit is good for the model to fit. Outcomes of the equation imply that the effects of A, C, A^2 are more important. The effect of the main and interactive effects of independent variables on the encapsulation efficiency was further studied by the perturbation and 3D response surface plots. The main influences of A, B and C on the encapsulation efficiency (R2) of rutin nanoparticles is illustrated in the perturbation plot (Figure 6a). This figure evidently expresses that R2 is mainly affected by B, followed by A&C which causes slight change on R2. 2D response surfaces, 3D contour plots, 3D cube plot and 2D interaction plot are used to establish the relationship between the dependent and independent variables, as shown in Figure 6b,c and d. R2 decreases from 75.17 to 58.16 % at low levels of A (Rutin). The encapsulation efficiency increases from 59.32 to 75.22 % at high levels of A.

The precise model made for % CDR at 12^{th} hour (R3) was discovered to be substantial with F-value of 641.99 ($p < 0.0001$) and R^2 value of 0.9988. A, B and C which are the independent variables has significant effects on the % CDR at 12^{th} hour. The model is significant as the P-values less than 0.0500 and this is indicated in Table 7. The Lack of Fit F-value of 3.17 implies the Lack of Fit is not significant relative to the pure error. There is a 14.70% chance that a Lack of Fit F-value this large could occur due to noise. Non-significant lack of fit is good to fit model. A, C, AB, BC, A^2, C^2 are significant models in this. The major effects of A, B and C on the percentage CDR (R3) of rutin nanoparticles are illustrated in the perturbation plot, where B has the major effect on R2 as compared to A and C (Figure 8a). The relationship between the dependent and independent variables was further investigated by 2D response surfaces, 3D contour plots, 3D cube plot and 2D interaction plot shown in Figure 8b,c and d.

The precise model made for PDI (R4) is significant. The F-value is 87.98 ($p < 0.0001$) and the R^2 value is 0.9912. This model is significant as the P-values less than 0.0500 (Table 8). The Lack of Fit F-value of 25.75 implies the Lack of Fit is significant. There is only a 0.45% chance that a Lack of Fit F-value this large could occur due to noise. Response surface plots, 2D response surfaces, 3D contour plots, 3D cube plot and 2D interaction plot are used to study the relationship between the dependent and independent variables as in Figure 9b,c and d. Figure 9a demonstrates the interactive effect of A and B on the PDI (R4). R4 increases from 0.261 to 0.348 when A is at low levels and increases from 0.256 to 0.412 when A is at high levels.

Table- 4: ANOVA results of the quadratic model for the response encapsulation efficiency (R2)

Source variations	Sum of Squares	DF	Mean Square	F Value	p-value Prob> F	
Model	616.17	9	68.46	543.18	< 0.0001	Significant
A-Rutin	0.9045	1	0.9045	7.18	0.0316	
B-PLA	540.55	1	540.55	4288.62	<0.0001	
C-Frequency	0.1891	1	0.1891	1.5	0.2602	
AB	0.3080	1	0.3080	2.44	0.1620	
AC	2.82	1	2.82	22.39	0.0021	
BC	0.3080	1	0.3080	2.44	0.1620	
A^2	1.92	1	1.92	15.20	0.0059	
B^2	70.19	1	70.19	556.90	<0.0001	
C^2	0.1937	1	0.1937	1.54	0.2550	
Residual	0.8823	7	0.1260			

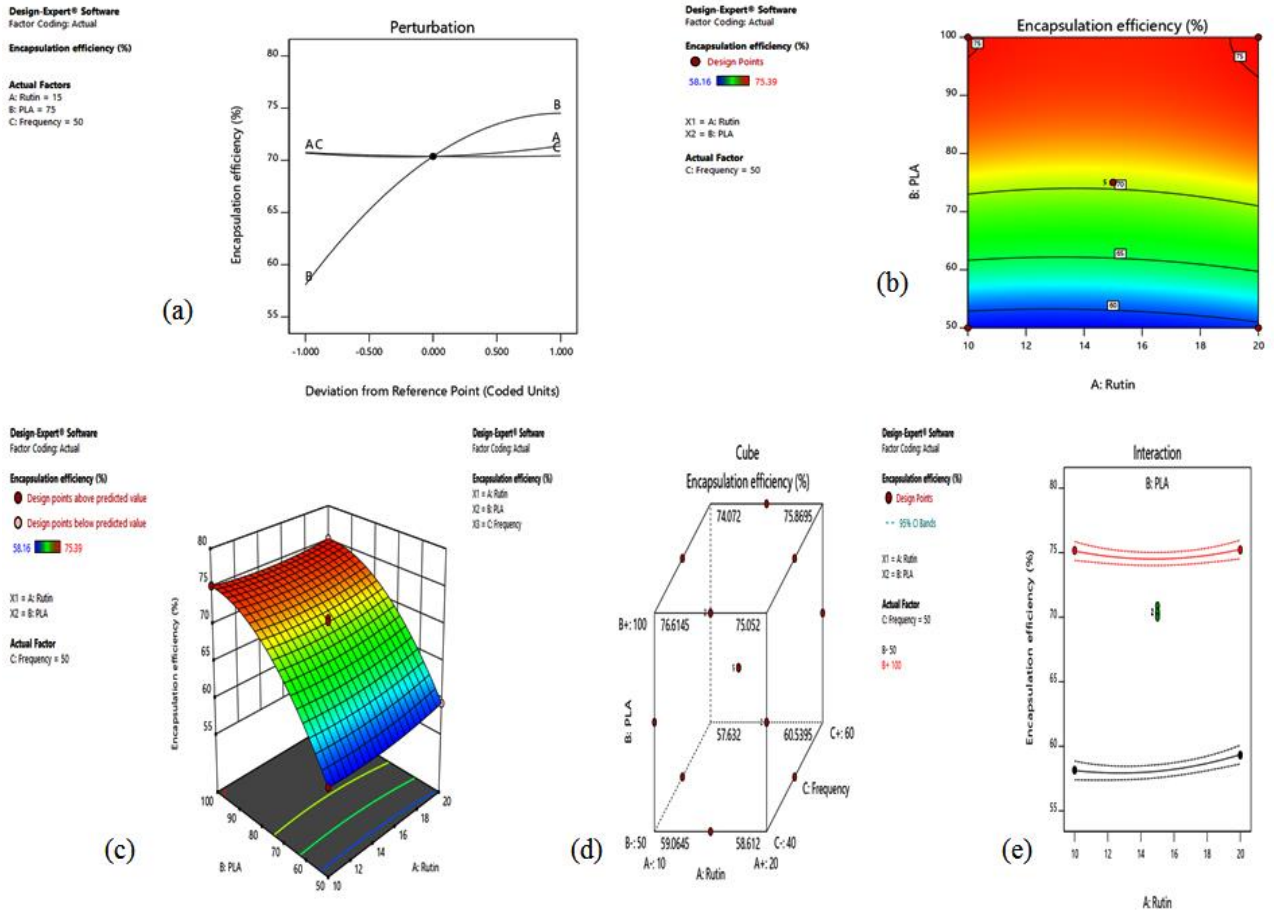

Figure-6: (a) Perturbation plot showing the main effect of Rutin (A), PLA (B) and frequency (C) on encapsulation efficiency (R2). (b) 2D Response surface plot presenting the interaction between the rutin and PLA affecting the encapsulation efficiency (R2). (c) 3D Response surface plot presenting the interaction between the rutin and PLA affecting the encapsulation efficiency (R2). (d) 3D cube plot of Box-Behnken design (R2). (e) 2D Interaction plot presenting the interaction between the rutin and PLA affecting the encapsulation efficiency (R2).

Table- 7: ANOVA results of the quadratic model for the response CDR at 12th hour (R3)

Source variations	Sum of Squares	DF	Mean Square	F Value	p-value Prob> F	
Model	142.47	9	15.83	641.99	< 0.0001	significant
A-Rutin	0.0903	1	0.0903	3.66	0.0972	
B-PLA	139.28	1	139.28	5648.42	<0.0001	
C-Frequency	0.3003	1	0.3003	12.18	0.0101	
AB	0.3080	1	0.3080	12.49	0.0095	
AC	0.0484	1	0.0484	1.96	0.2039	
BC	0.0156	1	0.0156	0.6337	0.4522	
A^2	0.3161	1	0.3161	12.82	0.0090	
B^2	1.91	1	1.91	77.46	<0.0001	
C^2	0.3278	1	0.3278	13.29	0.0082	
Residual	0.1726	7	0.0247			

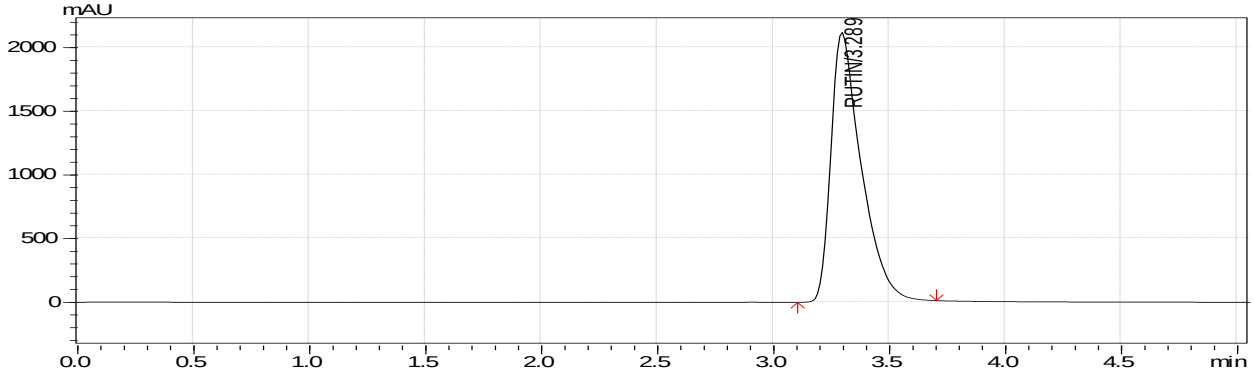

Figure-7: Typical HPLC chromatogram

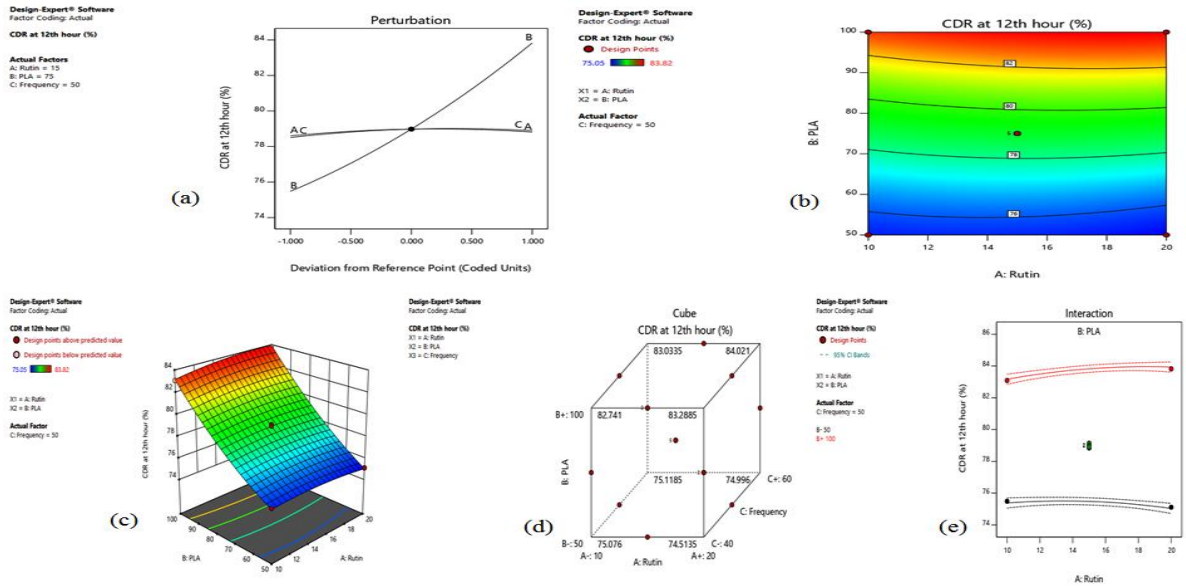

Figure-8: (a) Perturbation plot showing the main effect of rutin (A), PLA (B) and frequency (C) on % CDR at 12th hour (R3). (b) 2D Response surface plot presenting the interaction between the rutin and PLA affecting the % CDR at 12th hour (R3). (c) 3D Response surface plot presenting the interaction between the rutin and PLA affecting the % CDR at 12th hour (R3). (d) 3D cube plot of Box-Behnken design (R3). (e) 2D Interaction plot presenting the interaction between the rutin and PLA affecting the CDR at 12th hour (R3).

Table- 8: ANOVA results of the quadratic model for the response PDI (R4)

Source variations	Sum of Squares	DF	Mean Square	F Value	p-value Prob> F	
Model	0.0579	9	0.0064	87.98	< 0.0001	significant
A-Rutin	0.0002	1	0.0002	2.73	0.1422	
B-PLA	0.0161	1	0.0161	220.28	< 0.0001	
C-Frequency	0.0001	1	0.0001	1.64	0.2408	
AB	0.0005	1	0.0005	6.32	0.0402	
AC	0.0230	1	0.0230	313.83	< 0.0001	
BC	0.0001	1	0.0001	1.11	0.3276	
A^2	0.0019	1	0.0019	25.87	0.0014	
B^2	0.0129	1	0.0129	177.01	< 0.0001	
C^2	0.0018	1	0.0018	24.08	0.0017	
Residual	0.0005	7	0.0001			

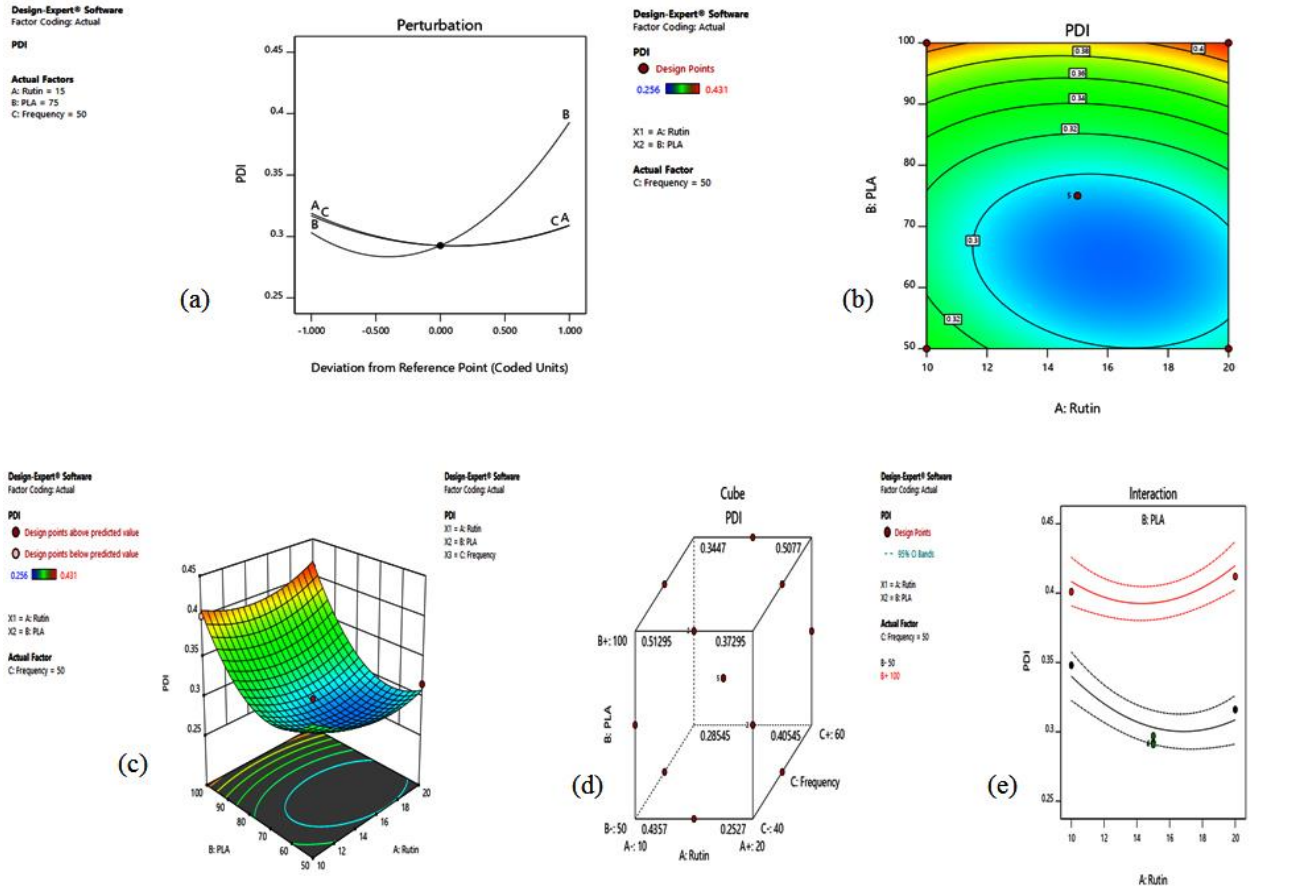

Figure-9: (a) Perturbation plot showing the main effect of rutin (A), PLA (B) and Frequency (C) on PDI (R4). (b) 2D Response surface plot presenting the interaction between the rutin and PLA affecting the PDI (R4). (c) 3D Response surface plot presenting the interaction between the rutin and PLA affecting the PDI (R4). (d) 3D cube plot of Box-Behnken design (R4). (e) 2D Interaction plot presenting the interaction between the rutin and PLA affecting the PDI (R4).

R5, R8 and R10 batches code of rutin nanoparticles were formulated according to the optimized levels after the polynomial equations relating the independent and dependent variables was constructed. The conditions of optimization were acquired by setting constraints on both the independent and dependent variables. The observed values were close to the expected values of the optimized process. This was described in Table 9 and 10.

Table- 9: Predicted values

Independent variable	Values	Predicted values			
		Particle size (nm)	Encapsulation efficiency (%)	CDR at 12th hour (%)	PDI
Rutin	15	240.596	70.376	78.978	0.2926
PLA	75				
Frequency	50				

Table- 10: Observed values

Code	Observed values			
	Particle size (nm)	Encapsulation efficiency (%)	CDR at 12th hour (%)	PDI
R5	241.63	70.88	79.01	0.292
R8	240.15	70.01	78.91	0.291
R10	241.09	70.37	78.99	0.291

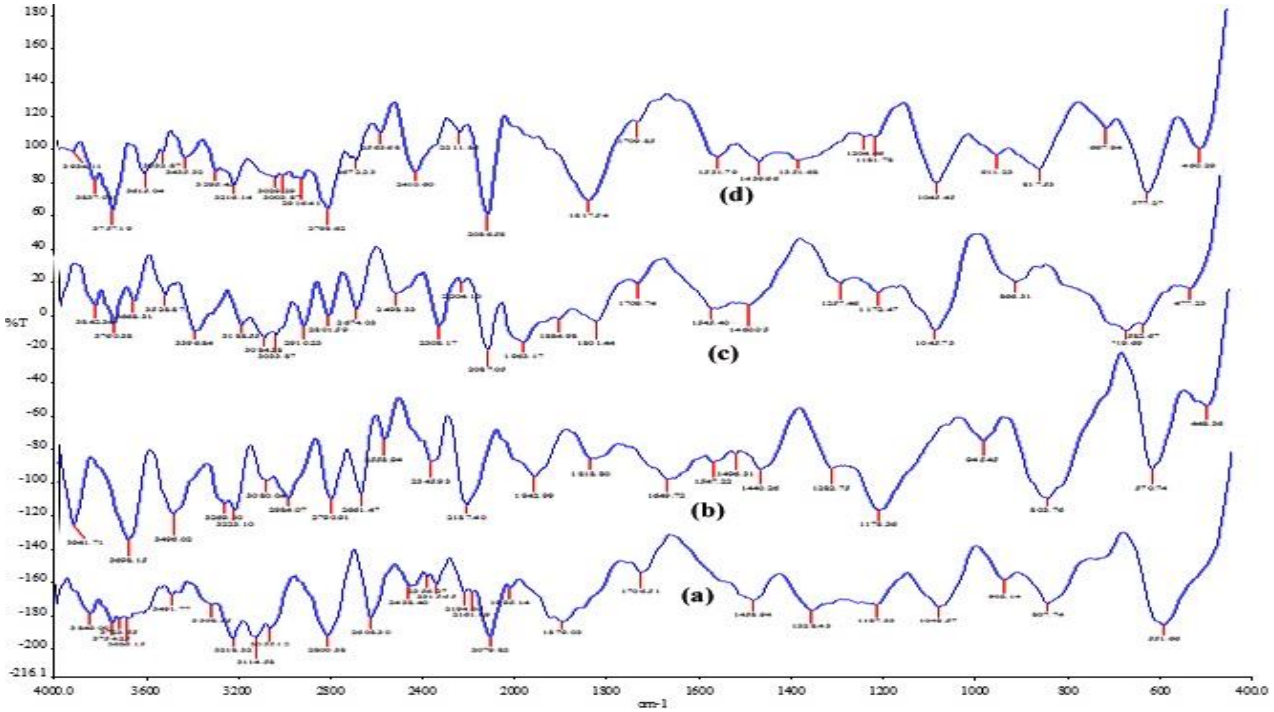

Figure-10: (a) FTIR spectrum of rutin. (b) FTIR spectrum of PLA. (c) FTIR spectrum of physical mixture of rutin and PLA. (d) FTIR spectrum of PLAcomposite nanoparticle.

Fig. 10a,b,c and d shows the FT-IR spectra of pure rutin, pure PLA, physical mixture of rutin &PLA, and PLAcomposite Nanoparticle. The spectrum of pure rutin showed principal peaks at wavenumbers (cm^{-1}) of 3849.00, 3754.25, 3723.55, 3686.15, 3491.77, 3308.55, 3218.32, 3114.58, 3055.12, 2800.38, 2608.30, 2438.40, 2356.27, 2315.65, 2194.30, 2161.89, 2079.82, 1995.14, 1879.03, 1706.51, 1458.94, 1328.43, 1187.33, 1048.57, 902.14, 807.74 and 551.66. The spectrum of pure PLA shows peaks at wavenumbers (cm^{-1}) of 3941.71, 3698.15, 3496.02, 3269.30, 3223.10, 3080.04, 2984.07, 2790.91, 2661.47, 2558.94, 2345.93, 2187.40, 1942.99, 1818.80, 1649.72,

1547.22, 1496.31, 1440.26, 1282.75, 1178.36, 945.45, 803.76, 570.74, 448.36.The physical mixture of rutin and PLA shows peaks at wavenumbers ($cm^{-}1$) at 3842.34, 3760.38, 3668.31, 3528.87, 3396.84, 3188.55, 3084.38, 3033.87, 2910.23, 2801.59, 2674.03, 2498.33, 2308.17, 2204.10, 2087.05, 1963.17, 1884.98, 1801.44, 1709.74, 1545.40, 1460.05, 1257.46, 1172.47, 1045.73, 866.31, 619.69, 582.67, 477.23.The peaks shown by rutin nanoparticle are at wavenumbers 3943.11, 3837.08, 3757.19, 3615.04, 3532.87, 3435.32, 3295.45, 3216.14, 3029.29, 3003.87, 2916.41, 2798.62, 2672.23, 2563.68, 2410.60, 2211.86, 2086.58, 1817.54, 1709.85, 1531.79, 1439.66, 1351.68, 1204.66, 1181.78, 1045.45, 911.23, 817.53, 667.94, 577.27, 460.29 $cm^{-}1$. Rutin compound formed the polymer active with no disturbance in the functional group. Hence, a polymerized active constituent has no change in effect after polymerization.

The morphology and size distribution of the rutin nanoparticles was analyzed using scanning electron microscopy (SEM). Images of nanoparticles prepared by single emulsion solvent evaporation technique. spherical shaped particles in nanosize range can be observed in Figure 11 and 12.

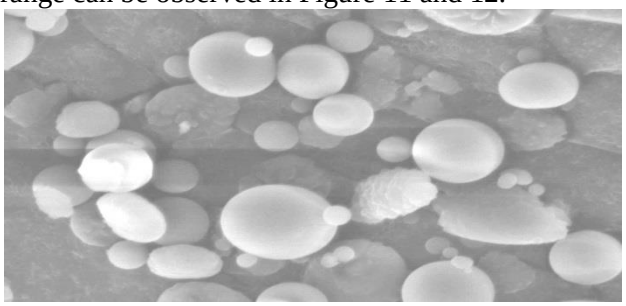

Figure -11: SEM image of PLAcomposite nanoparticle

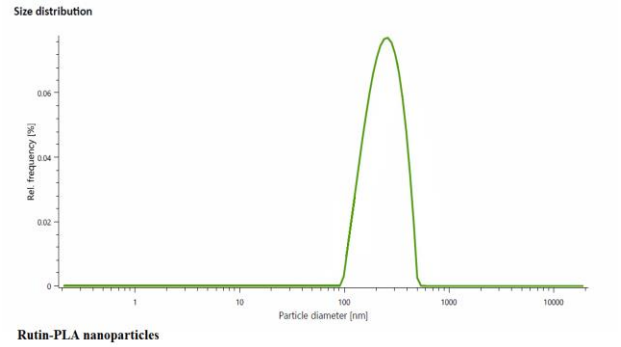

Figure-12: Size distribution of PLA composite nanoparticle

CONCLUSION

In this study, neat PLA composite nanoparticles were success-fully prepared via a solvent evaporation technique. SEM images showed uniform morphology of the nanoparticles with an average diameter range of 233.61–259.48nm. Rutin loaded PLA nanoparticles were fabricated and analyzed. The parameters examined were particle size, encapsulation efficiency, CDR at 12^{th} hour and PDI. Optimization was done based the results obtained and the results of the prepared PLA composite nanoparticles coincide with the expected values of various parameters.

REFERENCES

[1] R Mauludin, RH Müller, CM Keck. Development of an oral rutin nanocrystal formulation. *Int J Pharm*.370(1–2):202–9 (2009).

[2] R Kamel, M Basha & SH Abd El-Alim. Development of a novel vesicularsystem using a binary mixture of sorbitan monostearate and polyethyleneglycol fatty acid esters for rectal delivery of rutin. *Journal of Liposome Research.*23(1):28–36 (2013).

[3] SN Park, MH Lee, SJ Kim & ER Yu. Preparation of quercetin andrutin-loaded ceramide liposomes and drug-releasing effect inliposome-in-hydrogel complex system. *Biochemical and Biophysical Research Communications.* 435(3): 361–366 (2013).

[4] G Berlier., L Gastaldi, S Sapino, I Miletto, E Bottinelli, D Chirio., et al. MCM-41 as a useful vector for rutin topical formulations: synthesis, characterization and testing. *International Journal of Pharmaceutics.* 457(1):177–186 (2013).

[5] AS Macedo, S Quelhas, AM Silva & EB Souto. Nanoemulsions for delivery of flavonoids: formulation and in vitro release of rutin as model drug. *Pharmaceutical Development and Technology.* 19(6): 677–680 (2014).

[6] D Löf, K Schillén & L Nilsson. Flavonoids: precipitation kinetics and interaction with surfactant micelles. *Journal of Food Science.* 76(3): N35–39 (2011).

[7] R Mauludin, RH Müller & CM Keck. Development of an oral rutinnanocrystal formulation. *International Journal of Pharmaceutics.* 370(1–2): 202–209 (2009).

[8] NM Khalil, TC do Nascimento, DM Casa, LF Dalmolin, AC de Mattos,I Hoss, MA Romano, RM Mainardes, Pharmacokinetics of curcumin-loaded PLGA and PLGA-PEG

blend nanoparticles after oral administration in rats. *Coll. Surf. B Biointerface*. 101:353-360 (2013).

[9] SH Suhaimi, R Hasham, NA Roslic. Effects of formulation parameters on particle size and polydispersity index of orthosiphon stamineus loaded nanostructured lipid carrier. *Journal of Controlled Release.* 60:197-188 (1999).

[10**]** CA De Oliveira, DDA Peres, F Graziola, NAB Chacra, GLB De Araújo, AC Flórido., et al. Cutaneous biocompatible rutin-loaded gelatin-based nanoparticles increase the SPF of the association of UVA and UVB filters. *Eur J Pharm Sci*. 1;81:1-9 (2016).